Entanglement sharing in one-particle states

Arul Lakshminarayan[1,2,*] and V. Subrahmanyam[1,†]
[1]*Department of Physics, Indian Institute of Technology, Kanpur 208016, India*
[2]*Physical Research Laboratory, Navrangpura, Ahmedabad 380009, India*
(Received 4 December 2002; revised manuscript received 18 February 2003; published 19 May 2003)

Entanglement sharing among sites of one-particle states is considered using the measure of concurrence. These are the simplest in a hierarchy of number-specific states of many qubits and correspond to ''one-magnon'' states of spins. We study the effects of onsite potentials that are both integrable and nonintegrable. In the integrable case, we point to a metal-insulator transition that reflects on the way entanglement is shared. In the nonintegrable case, the average entanglement content increases and saturates along with a transition to classical chaos. Such quantum chaotic states are shown to have universal concurrence distributions that are modified Bessel functions derivable within random matrix theory. Time-reversal breaking and time-evolving states are shown to possess significantly higher entanglement sharing capacity than eigenstates of time-reversal symmetric systems. We use the ordinary Harper and the kicked Harper Hamiltonians as model systems.

DOI: 10.1103/PhysRevA.67.052304 PACS number(s): 03.67.Mn, 05.45.Mt

I. INTRODUCTION

Entanglement is a property of quantum systems, which sets it apart from those that are classical. Although it has been recognized as such from the early days of quantum mechanics, a spurt of understanding entangled states, both mathematically and generating them experimentally, has occurred in the past few years. Due to its potential as a resource in various tasks of quantum-information processing, it has moved from philosophical debates to the center stage of a large body of concrete work. For a recent review on the ideas involved, we refer to Ref. [1].

Entanglement within pure states of a bipartite system can be measured by the von Neumann entropy of the reduced density matrices. For a mixed state, while the entanglement can be measured as the average entanglement of its pure-state decomposition, the existence of an infinite number of such decompositions makes their minimization over this set a nontrivial task. Hill and Wootters [2] carried out such a procedure for the case of two two-state (qubit) systems and showed that a new quantity they called concurrence was a measure of entanglement. This facilitated the study of entanglement sharing among many qubits. One view of quantum entanglement, as a correlation that is much stronger than any other that is classical, is borne out here as two maximally entangled qubits cannot be entangled with any other; they will necessarily have to give up some of their correlation in order to share it with a third. At this stage, the nature of entanglement sharing among many-qubits is being studied intensively. Results are known for specific subsets of states in the many qubit Hilbert spaces [3]. A recent work has explored entanglement sharing among higher-state (higher than qubits) systems [4].

Due to the possibility of using spins as qubits in quantum computers, there have been many studies on the eigenstates of well-known spin Hamiltonians such as the Heisenberg model, Ising model in a transverse field, etc. [3,5], and related itinerant fermion systems [6]. There has been a conjecture that for complex quantum systems, entanglement will be an indicator of quantum phase transitions [7,8]. While these latter works have explored complexity from the viewpoint of many-particle, thermodynamic systems, few-particle systems that are classically chaotic are also complex in their own way with well-studied spectral transitions occurring in the quantum systems [9,10]. For bipartite systems of this kind, a pure-state entanglement has been shown to be sensitive to the presence of classical chaos, and the typical value of entanglement has been calculated from random matrix theory (RMT), including the distribution of the eigenvalues of the reduced density matrices [11–13].

In this paper, we study states in the simplest subspace of the 2^N-dimensional Hilbert space of N qubits, the N-dimensional subspace spanned by vectors with only one qubit in a different state from the rest, in some fixed single-qubit basis. These are the ''single-particle states'' within which we calculate entanglement sharing amongst the N qubits. Thus we think of a one-dimensional chain of N sites with a single-particle hopping among these. The entanglement among the qubits is then the entanglement among the sites themselves. We will use the (spinless) fermion language, since the connection between the fermion operators and the spin-half algebra of Pauli matrices is established through the Jordan-Wigner transformation [14]. Although, we do not need to use these here due to our restriction to single-particle states, the extension to higher number of particles then becomes straightforward.

In the integrable case, we show how the onsite potential can decrease the average entanglement present in a state and point to a sharp fall that can be identified in the Harper Hamiltonian to a metal-insulator transition. In the nonintegrable case, we show that the average entanglement content increases and saturates along with a classical transition to complete chaos. Simultaneously, near-neighbor entanglement gets destroyed and distant qubits start to get significantly entangled. The effect of time-reversal symmetry breaking is significant and leads to a larger entanglement content in the

*Email address: arul@prl.ernet.in; URL: http://www.prl.res.in/~arul
†Email address: vmani@iitk.ac.in

state. Random matrix theory is then used to explain these features and is shown to be successful in predicting the distribution of concurrence in an ensemble of chaotic states.

II. PRELIMINARIES

In this section, we collect results that set the formalism and notation. For completeness we first recall the definition of concurrence. Consider a bipartite composite system of subsystems A and B. A pure state $|\psi\rangle$ of the composite system is separable if it can be written as an outer product of states from A and B. In general, this is possible only if the reduced density matrix, after tracing out either A or B is itself a pure-state density matrix. Thus, the von Neumann entropy of the reduced density matrices is a measure of how entangled the pure state $|\psi\rangle$ is, and this is also the Shannon entropy of the state in the Schmidt decomposed form [15]. The entanglement $E(|\psi\rangle)$ in this case is defined to be the von Neumann entropy of the subsytems described by ρ_A or ρ_B, which are obtained by tracing out the states corresponding to subsystems B and A, respectively,

$$E(|\psi\rangle) = -\mathrm{tr}(\rho_A \log_2(\rho_A)) = -\mathrm{tr}(\rho_B \log_2(\rho_B)). \tag{1}$$

For bipartite density matrices, the measures of entanglement are not so easily calculable. The entanglement of formation for a general state ρ^{AB} is defined in the following way. For a given decomposition of the mixed state in terms of ensembles of pure states $|\psi_i\rangle$ specified with probabilities p_i,

$$\rho^{AB} = \sum_i p_i |\psi_i\rangle\langle\psi_i|, \tag{2}$$

one may find the average entanglement present in all the pure states involved. The entanglement of formation is then defined as the minimum of this average over all such possible pure-state decompositions:

$$E(\rho^{AB}) = \min \sum_i p_i E(|\psi_i\rangle). \tag{3}$$

This is one of the measures of entanglement, and is called the entanglement of formation, since it refers to the optimal ability to form such mixed states from maximally entangled pure states using only local operations on subsystems A and B and classical communication between them [16]. For a general bipartite mixed state, no explicit equation is known for this quantity. For a pair of qubits, Wootters [2] found such an expression that enables one to calculate the entanglement of formation from a knowledge of ρ^{AB}, which we recall for completeness.

Defining a spin-flip operator, which takes $\rho^{AB} \equiv \rho$ to

$$\tilde{\rho} = (\sigma_y \otimes \sigma_y)\rho^*(\sigma_y \otimes \sigma_y), \tag{4}$$

the concurrence of ρ is defined to be

$$C(\rho) = \max\{\sqrt{\lambda_1} - \sqrt{\lambda_2} - \sqrt{\lambda_3} - \sqrt{\lambda_4}, 0\}, \tag{5}$$

where λ_i are the eigenvalues of the non-Hermitian matrix $\rho\tilde{\rho}$. Wootters [2] showed that the entanglement of formation of ρ^{AB} is a monotonic function of its concurrence, and that as the concurrence varies over its possible range $[0,1]$, the entanglement of formation also varies from 0 to 1; thus concurrence is itself a good measure of entanglement.

For eigenstates of the number operator, as we will consider in this paper, the reduced density matrix of two sites has a special form that has already been studied and exploited in the literature. We recall for convenience the structure of these. Consider the N fermion density operator ρ that commutes with the number operator $\hat{N} = \sum_{i=1}^{N} \hat{c}_i^\dagger \hat{c}_i$. The site occupation basis is

$$|n_1, n_2, \ldots, n_N\rangle = c_1^{\dagger n_1} c_2^{\dagger n_2} \cdots c_N^{\dagger n_N} |0\rangle, \tag{6}$$

where $n_i = 0,1$ and $|0\rangle$ is the vacuum. Note that there is an isomorphism between these states and the states of N qubits. Consider the reduced density matrix ρ_{ij}^R of two sites i and j, where without loss of generality we can assume $i < j$. Due to the restriction that $\sum_{i=1}^{N} n_i = m$, this operator has the form:

$$\rho_{ij}^R = \begin{pmatrix} v_{ij} & 0 & 0 & 0 \\ 0 & w_{1ij} & z_{ij}^* & 0 \\ 0 & z_{ij} & w_{2ij} & 0 \\ 0 & 0 & 0 & u_{ij} \end{pmatrix}. \tag{7}$$

Here

$$v_{ij} = \langle (1-\hat{n}_i)(1-\hat{n}_j) \rangle, \tag{8}$$

$$u_{ij} = \langle \hat{n}_i \hat{n}_j \rangle, \tag{9}$$

$$w_{1ij} = \langle (1-\hat{n}_i)\hat{n}_j \rangle, \tag{10}$$

$$w_{2ij} = \langle \hat{n}_i (1-\hat{n}_j) \rangle, \tag{11}$$

$$z_{ij} = \left\langle \hat{c}_j^\dagger \hat{c}_i \prod_{l=i+1}^{j-1} (1-2\hat{n}_l) \right\rangle, \tag{12}$$

and $\langle \hat{A} \rangle = \mathrm{tr}(\hat{A}\rho)$. The entanglement between the sites (or qubits) i and j is measured here by the concurrence between them, which is given by

$$C_{ij} = C(\rho_{ij}^R) = 2 \max(|z_{ij}| - \sqrt{u_{ij} v_{ij}}, 0). \tag{13}$$

For the case $m = 1$, the single-particle subspace $u_{ij} = 0$ and the string of operators in the definition of z_{ij} is not there. If we write $|l\rangle = |0, \ldots, 1_l, \ldots, 0\rangle$, a general one-particle state is the superposition

$$|\alpha\rangle = \sum_{l=1}^{N} \phi_l^{(\alpha)} |l\rangle, \tag{14}$$

where $\phi_l^{(\alpha)} = \langle l|\alpha\rangle$. This then implies that the pairwise concurrence in this state are

$$C_{ij}^{\alpha}=2|\phi_i^{(\alpha)}\phi_j^{(\alpha)}|. \tag{15}$$

States that have a large minimum pairwise concurrence can be said to share entanglement better. As a gross but useful measure of entanglement sharing, we propose and study the average pairwise concurrence in a given state. For single-particle states, then

$$\langle C^{\alpha}\rangle=\frac{1}{d}\sum_{i<j}C_{ij}^{\alpha}=\frac{1}{d}\left(\left(\sum_{i=1}^{N}|\phi_i^{(\alpha)}|\right)^2-1\right), \tag{16}$$

where $d=N(N-1)/2$. From the structure of the average, we see that it has connections to measures of localization. In particular, the generalized entropies such as the Renyi entropy are related to the averaged concurrence. For a given discrete probability distribution $\{p_i, i=1,\ldots,N\}$, the Renyi entropy of order q is defined as

$$S_q^R[p]=\frac{1}{1-q}\ln\sum_{i=1}^{N}p_i^q. \tag{17}$$

This reduces to the usual information entropy as $q\to 1$.

Thus,

$$\langle C^{\alpha}\rangle=\frac{1}{d}[\exp(S_{1/2}^R)-1], \tag{18}$$

where $S_{1/2}^R$ is the Renyi entropy of order one-half. Therefore we expect that delocalized states share entanglement better, as an extreme case the site localized state $|l\rangle$ has zero average concurrence, as indeed it is a completely separable state. For a study connecting the Renyi entropy to localization we refer to [17]. It must be noted that we make this connection between localization and entanglement in the case of one-particle states; it remains to be seen if there is such a correspondence in the case of many-particle states.

We also note that $\langle C^{\alpha}\rangle\leqslant 2/N$. This implies that for one-particle states of qubits there cannot be states whose minimum pairwise concurrence exceeds $2/N$. This is the concurrence of isotropic states, which are defined by identical pairwise density matrices. It is not yet known if the above is true for states with larger number of particles [4].We go beyond the average and also study the *distribution* of concurrence, $p(C)$, in a given ensemble of states, which will be representative of single states. In principle then we can study various other averages of concurrence such as its square, etc., although we do not pursue this here.

We show that for eigenstates of quantized classically chaotic systems, the presence or absence of time-reversal symmetry, possibly a generalized time reversal, leads to very different distributions. Near-zero concurrence are improbable for eigenstates of time-reversal violating Hamiltonians, while they are most probable otherwise. Time-evolving states on the other hand, in either case, behave as the eigenstates of time-reversal violating Hamiltonians. We use, as a test model, the Harper Hamiltonian [18] (for a recent review and references, we point to Ref. [19]), which is an approximate model for electrons in a two-dimensional crystal subjected to a perpendicular magnetic field. This is a model with a rich spectral structure and a metal-insulator transition that continues to be studied from various viewpoints.

III. EFFECT OF ONSITE POTENTIALS

A. Integrable case

In this section, we study the effect of onsite potentials with a view of also comparing an integrable situation to a nonintegrable one, a more complex one to follow in the following section. We consider the Hamiltonian

$$\begin{aligned}H&=\frac{1}{2}\sum_{j=1}^{N}\hat{c}_j^{\dagger}\hat{c}_{j+1}+\frac{g}{2}\sum_{k=1}^{N}\hat{d}_k^{\dagger}\hat{d}_{k+1}+\text{H.c.}\\&=\sum_{j=1}^{N}\left[\frac{1}{2}(\hat{c}_j^{\dagger}\hat{c}_{j+1}+\text{H.c.})+g\cos(2\pi j/N)\hat{c}_j^{\dagger}\hat{c}_j\right].\end{aligned} \tag{19}$$

Here,

$$\hat{d}_k=\frac{1}{\sqrt{N}}\sum_{j=1}^{N}\exp(2\pi ikj/N)\hat{c}_j \tag{20}$$

is the Fourier transform of the site annihilation operator and k is a momentum index. We will assume periodic boundary conditions first: $\hat{c}_{N+1}=\hat{c}_1$, $\hat{d}_{N+1}=\hat{d}_1$. H is a one-dimensional Harper Hamiltonian with the onsite potential being $\cos(2\pi q)$. We can think of the large-N limit as approaching a flow on the unit torus, with the classical Hamiltonian

$$\cos(2\pi p)+g\ \cos(2\pi q), \tag{21}$$

and that we are considering its finite quantum mechanics with N states.

We briefly indicate the reasoning involved. Note that the operators

$$\hat{V}=\sum_{j=1}^{N}\hat{c}_{j+1}^{\dagger}\hat{c}_j,\quad \hat{U}=\sum_{k=1}^{N}\hat{d}_k^{\dagger}\hat{d}_{k+1} \tag{22}$$

are unitary translation operators on the states $|l\rangle$ and $|k\rangle\equiv\hat{d}_k^{\dagger}|0\rangle$: $\hat{V}|l\rangle=|l+1\rangle$ and $\langle k+1|=\langle k|U$. Thus, the site and the momentum states span a lattice on the conventional unit torus phase space with the translation operators V and U obeying a finite Weyl commutation relation; they are discrete versions of $\exp(-i\hat{p}a/\hbar)$ and $\exp(-i\hat{x}b/\hbar)$ (where a,b are phase space shifts), respectively [20]. The torus quantization implies the condition $\hbar=h/(2\pi)=A/(2\pi N)$, where $A=1$ is the area of the unit torus phase space. Also with $a=b=1/N$, a lattice translation unit in phase space, and with the eigenvalues of position and momentum being l/N and k/N, leads to the large-N or classical Hamiltonian as specified above.

Thus, we see that the original Hamiltonian is an integrable one in the classical limit, since it has only a single degree of freedom. From a Bethe-Ansatz perspective the integrability of this Hamiltonian is discussed in Ref. [21]. We can also now easily visualize the eigenstates of the Hamiltonian as being localized on the constant energy curves of the classical

Hamiltonian. Thus, although we cannot solve the eigenvalue problem analytically, we can understand the features of all the states involved.

Another modification of the Hamiltonian is the class where the onsite potential is incommensurate with the lattice, and herein the Harper Hamiltonian shows a rich structure which has been studied extensively. In particular, we will modify the Hamiltonian to read

$$H=\sum_{j=1}^{N}\left[\frac{1}{2}(\hat{c}_j^{\dagger}\hat{c}_{j+1}+\text{H.c.})+g\cos(2\pi\sigma j/N)\hat{c}_j^{\dagger}\hat{c}_j\right], \tag{23}$$

where σ is a real incommensurability parameter. For σ/N that is a fixed irrational number (in the original Harper model, this is the ratio of the flux through a lattice cell to one flux quantum) as N tends to infinity a metal-insulator transition occurs at $g=1$ where the spectrum is a Cantor set.

First, the case $g=0$, $\sigma=1$ corresponds to an itinerant particle on the lattice and the eigenfunctions are simply the momentum states $|k\rangle$. These clearly have pairwise concurrence $2/N$ for all pairs and represent optimally delocalized states in the site basis as far as the concurrence go. Due to double degeneracy, however, there also exist eigenstates that have smaller entanglement. For $g>0$, $\sigma=1$, the classical Hamiltonian above provides us the well-known phase space of the Harper flow with two elliptic fixed points and two hyperbolic fixed points per cell. From the Hamiltonian we know that the energy eigenvalues are bounded by $-1-g \leqslant E \leqslant 1+g$. The classical phase space will consist of two separatrices corresponding to energies of the equilibrium points (0,1/2) and (1/2,0). Thus, we know that for $0<g<1$, the quantum states with energies in the range $-1+g<E<1-g$ are dominantly Kolmogorov-Arnold-Moser (KAM) rotational states that are spread along the sites with the edge states being separatrix states.

There are states that will be localized in the site basis corresponding to torus-quantized states around the elliptic fixed points, while the hyperbolic orbits will provide the separatrix states. When $g<1$, there are smooth phase-space curves along the momentum direction and the separatrices localize states in momentum, while at $g=1$ the two separatrices form a single diamond square, and for $g>1$ the separatrices tend to localize states along the position. It is evident that as $g\to\infty$, there are states that are completely site localized. Thus, the classical picture also singles out $g=1$ as a special point.

Thus, this elementary picture then indicates that as g increases, the average concurrence will tend to decrease. As a further gross measure we also average over all the states α in the spectrum, and show in Fig. 1 the decrease in the average concurrence ($\langle C\rangle$) as a function of g. Thus, onsite potentials decrease concurrence as they tend to localize states. The point $g=0$ has an exact double degeneracy, while the momentum states are eigenstates with the maximum concurrence of $2/N$, and as soon as $g>0$ this degeneracy is broken and the states are continuation of combinations of the degenerate states with smaller entanglement. As an effect, the apparent $g\to 0$ limit is smaller than 2 in Fig. 1.

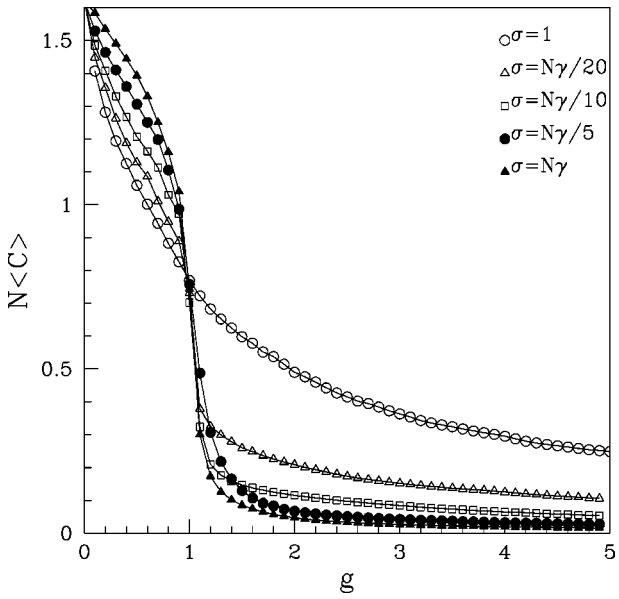

FIG. 1. Spectral averaged concurrence as a function of onsite potential strength for the Harper Hamiltonian. $N=101$ and $\gamma=(\sqrt{5}-1)/2$.

In the same figure, we also show the effect of σ. When σ is an irrational number larger than unity, the transition at $g=1$ becomes sharply visible. We note that the average concurrence decreases dramatically as g crosses unity, corresponding to a metal-insulator transition in the infinite incommensurate chain. This is again a reflection of the fact that wave functions change from a ballistic regime to an exponentially localized one. For rational values of σ close to these irrational values, a transition is still seen due to finite N effects. Thus, apart from quantum phase transitions, it is possible that the signature of entanglement will also be present in metal-insulator transitions.

Scaling behavior with the size of the lattice N is illustrated in Fig. 2, where a transition is seen from the scaling law $\langle C\rangle\sim N^{-1}$ for the metallic regime $g<1$ to $\langle C\rangle\sim N^{-2}$ for the insulating regime $g>1$. The scaling in the localized or insulating regime is intuitively reasonable, since there will be only a small number of significant components, and hence only number of pairs of order unity can be expected to have significant concurrence; hence, the average will go approximately as the inverse of the number of pairs. In the metallic regime there is a more democratic spread of concurrence and results in the $1/N$ scaling which we will later see to be the rule for chaotic and random states. At the critical point $g=1$, there does not seem to be a simple good power-law fit for the range of N (101–808) values used here, and while this warrants further study, we do not pursue this in this paper.

In Fig. 3 is shown the average concurrence in individual states of a given spectrum as a function of the energy of the state, appropriately scaled. For $g<1$, we see that there is a plateau of large concurrence corresponding to states on the rotational KAM invariant curves extending over all of the q space, while the edges are the separatrix states. The tails on either side correspond to states that are localized around the

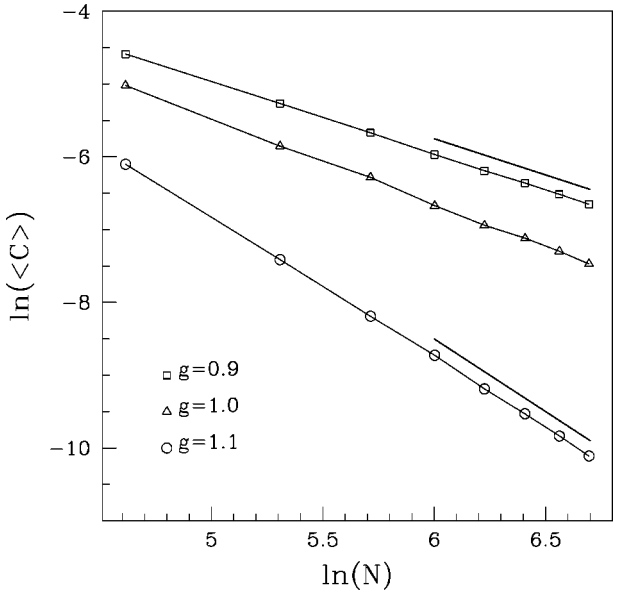

FIG. 2. Scaling of the spectral averaged concurrence with N for $\sigma = N\gamma$, $\gamma = (\sqrt{5}-1)/2$. Shown are three cases corresponding to metallic, critical, and insulating regimes, the short lines correspond to lines with slope 1 ($g=0.9$) and slope 2 ($g=1.1$).

elliptic fixed points and represent low-entanglement states on the average, having a tendency to form coteries. As g increases, the plateau gets squeezed out of existence and only the separatrix states remain at $g=1$. For larger g, the invariant curves between the separatrices extend over the momentum space rather than the position and tend to start localizing in the site basis. The very low concurrence states correspond to those that are spread in momentum maximally and therefore highly site localized.

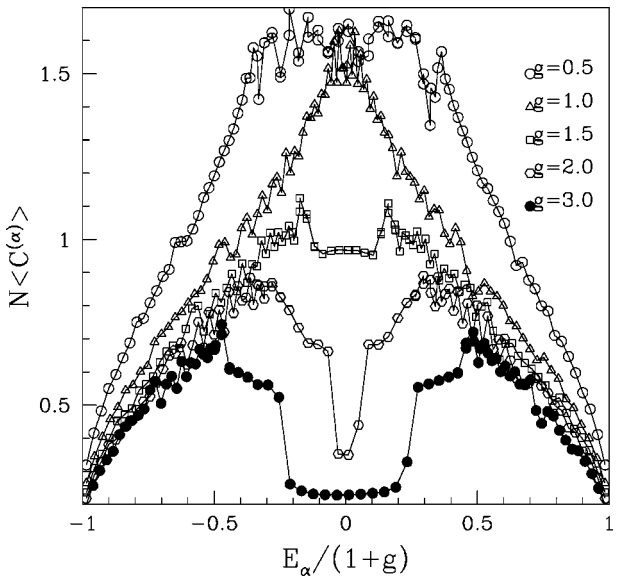

FIG. 3. Average concurrence in the individual states of the Harper Hamiltonian as a function of energy, with $N=101$, $\sigma=1$ at various values of the onsite potential.

B. Nonintegrable Hamiltonians

Nonintegrable Hamiltonians are the rule for systems with more than one degree of freedom, or for many-particle systems. While there are many important interacting models in condensed-matter physics such as the Heisenberg model for which entanglement sharing has been studied, the case of nonintegrability with the possibility of chaos has yet to be explored. We begin again with the simplest case of a single-particle spectrum. Building upon the Harper Hamiltonian that we have just discussed, the kicked Harper Hamiltonian then provides us with a suitable model. The fact that we wish to remain on a one-dimensional lattice means that we have to introduce a time-dependent onsite potential to introduce nonintegrability. The kick type of time dependence leads to simple models that have been extensively studied in the context of quantum chaos. It has been pointed out that similar models are of relevance in cyclotron resonance experiments in antidot arrays [22].

Thus, the Hamiltonian we will consider is

$$H=\sum_{j=1}^{N}\left[\frac{1}{2}(\hat{c}_j^{\dagger}\hat{c}_{j+1}+\text{H.c.}) + g\cos(2\pi j/N)\hat{c}_j^{\dagger}\hat{c}_j\sum_{n=-\infty}^{\infty}\delta(2\pi t/\tau-n)\right]. \quad (24)$$

A train of impulses is provided at intervals of time $\tau/(2\pi)$. As $\tau\to 0$, we recover the integrable Harper equations. Note that we have set for the nonintegrable case $\sigma=1$. The corresponding large-N, classical Hamiltonian is

$$H=\cos(2\pi p)+g\cos(2\pi q)\sum_{n=-\infty}^{\infty}\delta(2\pi t/\tau-n), \quad (25)$$

from which we get the canonical (area-preserving) map of the unit torus to itself connecting phase-space variables immediately after two consecutive impulses

$$q_{n+1}=q_n-\tau\sin(2\pi p_n),$$
$$p_{n+1}=p_n+\tau g\sin(2\pi q_{n+1}). \quad (26)$$

This map has been studied extensively and develops full fledged chaos for large τ [23]. For completeness, we illustrate this transition to classical chaos in Fig. 4, fixing $g=1$ as in the subsequent calculations, too.

As is standard, the Floquet operator (quantum map) connecting states just after impulses is the quantum propagator

$$\hat{U}(\tau)=\exp[-i\tau g\cos(2\pi\hat{q})/h]\exp[-i\tau\cos(2\pi\hat{p})/h]. \quad (27)$$

With $h=1/N$, we get the quantum version in the basis spanned by the site-localized states $|l\rangle$. The spectrum of the Floquet operator is then of interest. We study the average concurrence and the distribution of concurrence in the eigenstates of the above quantum map. The spectra of quantized chaotic systems are very sensitive to whether time-reversal (TR) symmetry is present or not. However, it was seen in

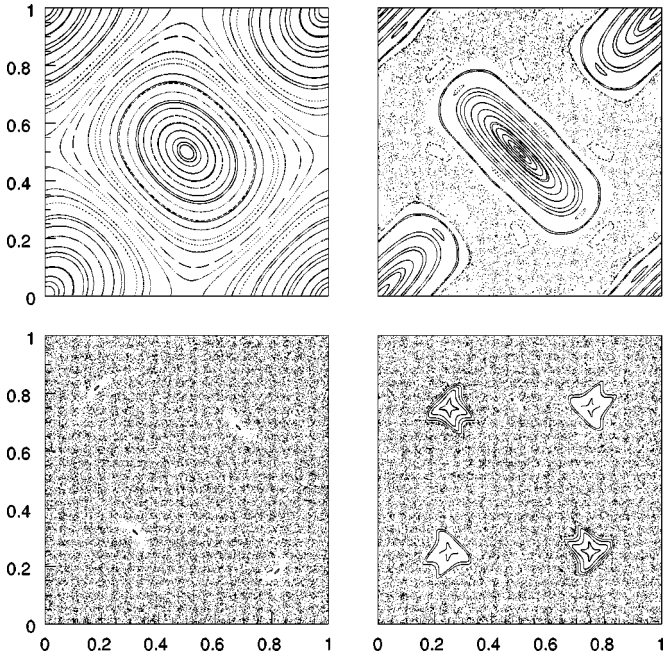

FIG. 4. The phase space (q,p) of the classical map for $g=1$ and $\tau=0.1$, 0.3, 0.5, and 0.7 clockwise from top left.

Ref. [12] that the entanglement in pure states of bipartite chaotic systems, consisting of Hilbert spaces of large dimensions, is not sensitive to TR symmetry. This is because only the density of eigenvalues of the reduced density matrix determines the entanglement in the case studied there. We will see below that concurrence sharing among many qubits is affected crucially by this symmetry. To show this, we change the boundary condition on the states $|l\rangle$ and introduce a phase, or equivalently change the boundary conditions on the site creation operators

$$|l+N\rangle=\exp(-2\pi i\beta)|l\rangle; \quad c^{\dagger}_{l+N}=\exp(-2\pi i\beta)c^{\dagger}_{l}, \tag{28}$$

where $0<\beta<1/2$. This shifts the momentum eigenvalues to $(k+\beta)/N$. We retain periodic boundary conditions on the momentum states $|k\rangle$, and note that in this kinematic framework the momentum-site transformation is the Fourier transform

$$\hat{d}_k=\frac{1}{\sqrt{N}}\sum_{j=1}^{N}\exp[2\pi i(k+\beta)j/N]\hat{c}_j. \tag{29}$$

The phase β is like a magnetic flux line threading the periodic chain, which is a standard way to break the TR symmetry.

In Fig. 5 the average concurrence is shown as a function of τ for various values of the TR breaking phase β. For any value of this phase, it is clear that along with a transition to classical chaos there is an increase in the average pairwise concurrence, and this corresponds to an increasing delocalization of the states. The concurrence sharing saturates after a transition to classical chaos, at around $\tau=0.6$, and we expect that in this regime, RMT will be able to model the concurrence, we show below that this expectation is borne out.

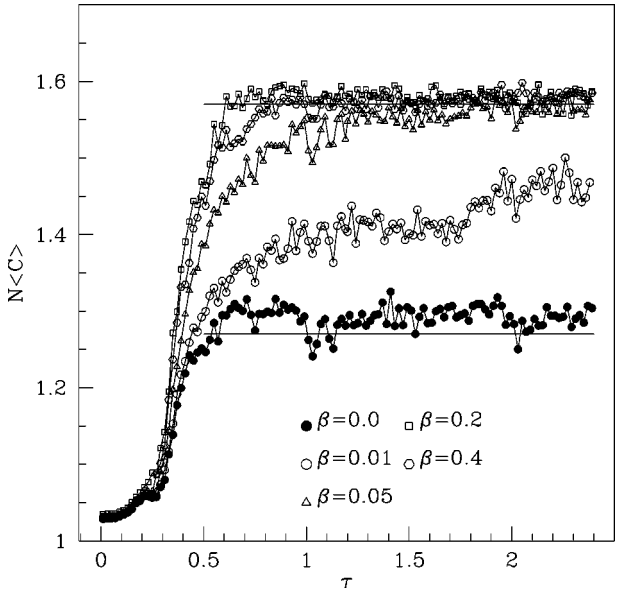

FIG. 5. Spectral averaged concurrence as a function of τ for the kicked Harper Hamiltonian. Shown are both the TR symmetric ($\beta=0$) and several non-TR symmetric cases ($\beta\neq 0$) and $N=101$. The horizontal lines correspond to the RMT averages $4/\pi$ and $\pi/2$, respectively.

It is also clear from this figure that breaking TR symmetry leads to significantly larger entanglement sharing. The effect of time-reversal breaking is pronounced in the chaotic regime since the delocalized states experience the changed boundary conditions. In this figure we also show how sensitive the TR breaking is by changing the phase only slightly. For β greater than the dimensionless Planck's constant $1/N$, we see a universal saturation effect. It is interesting that as β decreases, the saturation seems to occur for larger τ which is also a region of larger classical chaos. We may conclude as a general principle that entanglement sharing is more effective in eigenstates of TR breaking Hamiltonians, and that this is a general principle in the context of one-particle states supported by an analysis using RMT below.

We state results for two universality classes of RMT relevant here, namely, from the Gaussian unitary ensemble (GUE) for time-reversal breaking Hamiltonians, and the Gaussian orthogonal ensemble (GOE) for TR preserving, spinless systems [10,24]. We quantify the above observations and note in advance, what we prove further on, that the average concurrence calculated from the RMT in the two cases are

$$\langle C^{\alpha}\rangle=\begin{cases}4/\pi N & \text{(GOE)}\\ \pi/2N & \text{(GUE).}\end{cases} \tag{30}$$

The saturation values of Fig. 5 agree well with these estimates from RMT, which are shown as horizontal lines. However, RMT seems to predict a somewhat smaller value than the observed average in the case when there is TR symmetry.

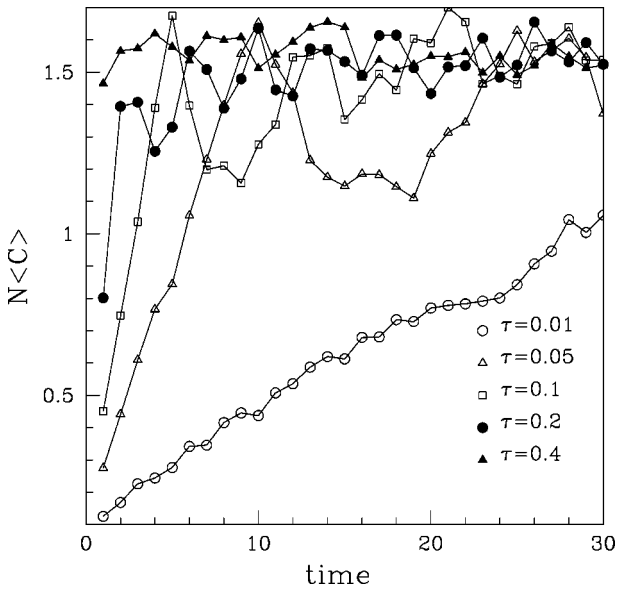

FIG. 6. Average concurrence for a nonstationary state (initially $|l=21\rangle$), as a function of time. $N=101$, and near integrable to chaotic cases are shown.

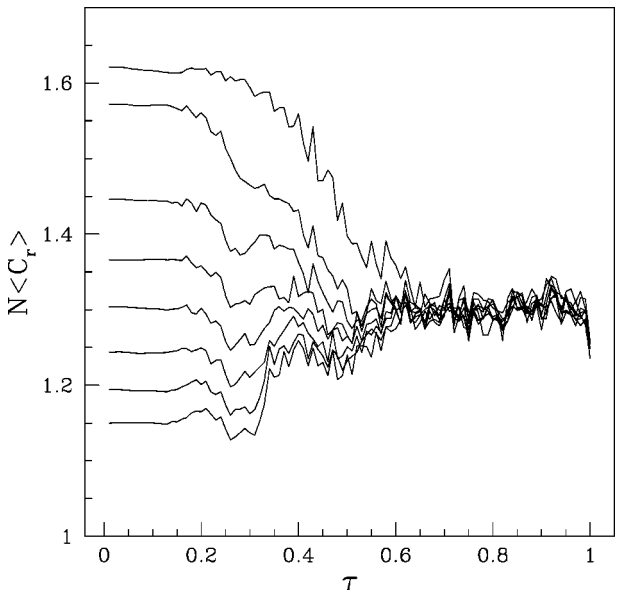

FIG. 7. Average rth-neighbor concurrence as function of τ for the kicked Harper Hamiltonian. From top to bottom, $r=1-15$ in steps of 2 and $N=101$ in all cases.

Note that the RMT result used above is a finite-N exact value. Phase-space localization effects on chaotic eigenfunctions due to classical periodic and homoclinic orbits do lead to significant deviations from RMT [26], however here it is interesting that the deviations seem to be more when there is TR symmetry. Concurrence could be a sensitive measure to study deviations of real eigenfunctions of quantized chaotic systems from RMT predictions; further study on this aspect is required.

The average concurrence promises in the case of the one-particle spectrum to be an interesting measure of localization. We also emphasize that these results are only dependent on the single-particle nature of the states and are *independent* of the dimensionality, although our models are one-dimensional. Calculations with different N not presented here also confirm further the RMT scaling $\langle C\rangle \sim N^{-1}$, which we also observed in the metallic regime of the integrable Harper Hamiltonian, and as in that case we postpone a more extensive scaling analysis.

Time evolution intrinsically involves complex vectors and therefore we expect that time-evolving states will share, under a quantum chaotic evolution, entanglement that is identical with that of TR breaking Hamiltonian eigenstates. This is borne out in Fig. 6 where several cases ranging from near integrable to chaotic are shown. The near-linear increase of the average concurrence in time for near-integrable systems is replaced by a rapid increase to the TR breaking average of $\pi/2N$ around which there are small fluctuations. The initial state in all these cases is a site-localized one with null entanglement. While the average pairwise concurrence of chaotic eigenstates is larger than that of regular states, it is reasonable to expect the opposite if one were to only include near-neighbor pairs of sites. We expect that the nearest neighbors are treated preferentially in regular states, while for random or chaotic states the connections from one site to another is also random. This expectation comes from the fact that regular states are smoother than the more fragmented structures one finds on a coarse scale for chaotic states. This is in turn related to tori quantization of regular states, as opposed to a situation more akin to superposition of random waves for chaotic states [9].

Thus, we define the rth-neighbor average concurrence

$$C_r^{(\alpha)}=\frac{1}{N}\sum_{i=1}^{N} C_{ii+r}^{(\alpha)}. \tag{31}$$

In Fig. 7 this is shown, after averaging over the spectrum α, for various r as a function of τ for TR symmetric eigenstates. It is clear that the correlation between near-neighbor pairs is indeed much stronger for regular states. There is a correlation length beyond which the entanglement falls below that of the random or chaotic states average of $4/\pi N$. This correlation length is then an interesting quantum length scale of the problem; we call this a quantum scale as it refers to the intrinsically quantum property of entanglement. In Fig. 8 we show how $C_r^{(\alpha)}$ falls as a function of r for various τ after averaging over the complete spectrum $\{\alpha\}$.

C. RMT and concurrence

In this section, we derive the averages stated and demonstrated above, as well as the *distributions* of the concurrence between sites of one-particle states using random matrices as models. The eigenfunction component distributions are derived within RMT by invoking a microcanonical distribution with the constraint being normalization. If $x_1, x_2, \ldots, x_d$ are real numbers distributed uniformly over the d-dimensional spherical surface of unit radius (normalization), the reduced density of l variables is given by [10]

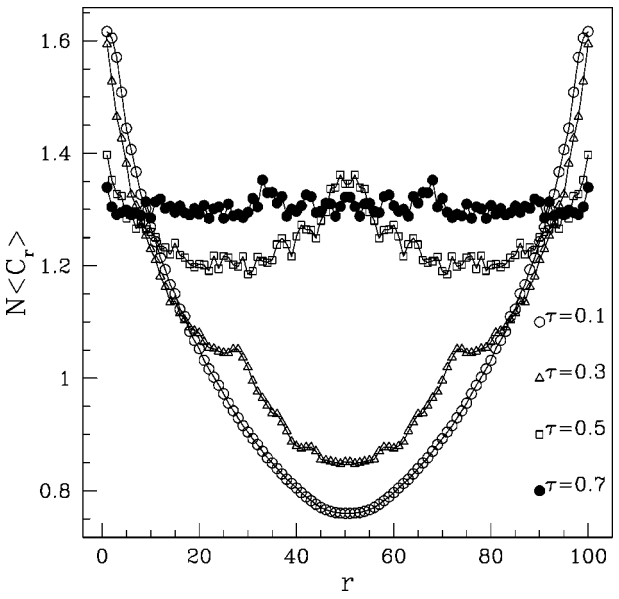

FIG. 8. Average rth-neighbor concurrence as function of r for the kicked Harper Hamiltonian. Shown are cases ranging from the near integrable to the chaotic. $N=101$ and $\beta=0$.

$$P^{(d,l)}(x_1,x_2,\ldots,x_l) = \pi^{-l/2}\frac{\Gamma(d/2)}{\Gamma((d-l)/2)}\left(1-\sum_{n=1}^{l}x_n^2\right)^{(d-l-2)/2}. \tag{32}$$

In the case of TR symmetric systems, there exist time-reversal adapted bases wherein the components of the eigenfunctions are real and these may then be taken to be the x_i above with $d=N$. In the case of TR breaking Hamiltonians, there are no such bases and the eigenfunctions are generically complex, in which case we identify the real and imaginary parts of the state components with the x_i and $d=2N$ [10]. Thus, the average concurrence for the GOE case, relevant for TR symmetric Hamiltonians, may be calculated as the integral,

$$\langle C\rangle = \int_{R_2} dx_1\, dx_2\, P^{(N,2)}(x_1,x_2)2\sqrt{x_1^2x_2^2} = 4/\pi N. \tag{33}$$

The region R_2 is the interior of the circle $x_1^2+x_2^2\leqslant 1$. For the GUE case, where the wave functions have complex components and $d=2N$, the average concurrence is

$$\langle C\rangle = \int_{R_4} dx_1\, dx_2\, dx_3\, dx_4\, P^{(2N,4)}(x_1,x_2,x_3,x_4) \times 2\sqrt{x_1^2+x_2^2}\sqrt{x_3^2+x_4^2} = \pi/2N. \tag{34}$$

The region R_4 is now the four-sphere volume: $x_1^2+x_2^2+x_3^2+x_4^2\leqslant 1$. These are the formulas stated in Eq. (30).

In order to calculate the distributions themselves, we choose to use the large N forms of the distributions when the components tend to become independent. Let $\rho(x)$ be a single-component distribution of $x=|\phi_j^{(\alpha)}|^2$. The distribution function $\rho(x)$ is known to be different for the two universality classes used here. The GOE distribution, the Porter-Thomas distribution, was first used in the study of nuclear resonance widths [25]:

$$\rho(x)=\begin{cases}\sqrt{N/2\pi x}\,\exp(-Nx/2) & \text{(GOE)}\\ N\,\exp(-Nx) & \text{(GUE).}\end{cases} \tag{35}$$

Thus, the concurrence distribution $p(C)$ is then straightforward to calculate for one-particle states. We state the distributions for the scaled concurrence $c=NC$,

$$p(c)=\int_0^\infty\int_0^\infty \delta(c-2N\sqrt{xy})\rho(x)\rho(y)dx\,dy. \tag{36}$$

The result is

$$p(c)=\begin{cases}(1/\pi)K_0(c/2) & \text{(GOE)}\\ cK_0(c) & \text{(GUE),}\end{cases} \tag{37}$$

where K_0 is the modified Bessel function that has a logarithmic divergence at the origin. The average concurrence, stated in Eq. (30) and derived above, also follow from the single-component distributions, i.e., at least in the averages there are no corrections coming from correlations between the components.

We recall that one-particle states that maximally share entanglement are those whose reduced density matrices for all the pairs are identical, such as the noninteracting case eigenstates states $\phi_j^{(k)}=\exp(2\pi ijk/N)/\sqrt{N}$. If we take the pairwise concurrence, $2/N$ in this case to be a marker, the fraction of pairs with concurrence larger than this is

$$\int_2^\infty p(c)dc = 0.21, 0.28 \tag{38}$$

for GOE, and GUE, respectively. Thus, a significant proportion of the pairwise concurrence in a one-particle random state is higher than $2/N$. For large c (practically greater than 2), the asymptotic distributions are

$$p(c)\sim e^{-c/2}/\sqrt{\pi c},\quad \sqrt{\pi c/2}e^{-c} \tag{39}$$

for the two cases of GOE and GUE, respectively.

In Fig. 9 we compare the distributions from RMT with numerical calculations. To do this we combine the pairwise concurrence of all the eigenstates into a concurrence ensemble. We see that there is an excellent agreement between the theory and numerical calculations, although there are discernible deviations for small concurrence. It must be noted that these distributions are *universal*; they are independent of system, except for the requirement of a classically chaotic limit. Thus, it is clear that TR symmetry could play a crucial role in the way entanglement is shared in a quantum state. Also the case of the Gaussian symplectic ensemble has not been considered here due to the additional complexity of a Kramer's degeneracy.

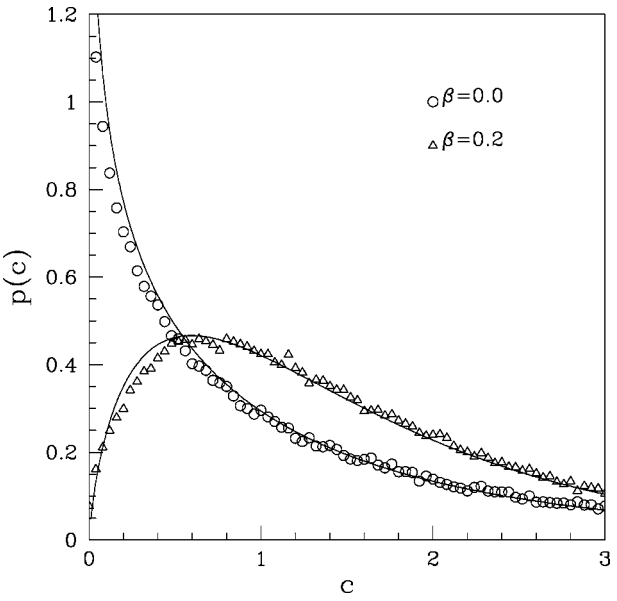

FIG. 9. The concurrence distributions for the kicked Harper Hamiltonian with $\tau=0.8$ and $N=101$. Shown using points are the cases of time-reversal preserving ($\beta=0$) and time-reversal breaking ($\beta=0.2$) Hamiltonians. The smooth curves are the RMT predicted distributions.

IV. CONCLUSIONS

We have studied entanglement sharing in one-particle states using the measure of concurrence. We have studied the average of the concurrence, spectral averaged concurrence, as well as the distribution of concurrence in a given state. Our attempt has been to begin studying the effect of nonintegrability and chaos in this interesting quantum measure that has possible applications in quantum-information theory. We have found that chaos in the corresponding quantum system implies that concurrence in individual one-particle states are distributed in a universal manner, which depends only on the presence or absence of TR symmetry. The absence of TR symmetry has been shown to lead to more entanglement sharing, and we have quantified these statements with the help of RMT.

Also a transition to chaos has been shown to accompany an increase in the spectral averaged concurrence. We expect that spectral averaging will have a small effect in the case of chaotic systems, while there will be much larger state to state fluctuations in the case of regular states. We have also made connections between the averaged concurrence and the measures of state localization such as the Renyi entropy, something that enables us to qualitatively understand the behavior of entanglement sharing in these states. For instance we have demonstrated that for regular states, near-neighbor concurrence is preferred, while for chaotic states there is no such metric preference. Due to the essential simplicity of the concurrence in one-particle states, we have been able to analyze details such as concurrence distributions. It is of much interest to see how many of the conclusions, for instance that concerning the role of TR symmetry, carry over to general states.

The effect of onsite integrable potentials has also been studied and it is noted that transitions such as metal-insulator transitions are reflected in the way entanglement is shared. It is shown that in the metallic regime, entanglement is shared better, while in the insulating regime, it is not. This is reasonable due to the connections between wave-function localization and concurrence noted above. Also the finite-size scaling of the concurrence in the metallic and insulating cases have been noted. A more detailed scaling analysis in all cases, including the critical point is warranted. The hypothesis that quantum-information theory will be an approach to study ''complex'' quantum systems [27] is borne out here in the context of entanglement and single-particle chaos. The way in which many-particle states differ are significant and ongoing work on this will soon be reported.

ACKNOWLEDGMENTS

A.L. thanks Professor M. K. Verma and other members of the Department of Physics, IIT Kanpur, for their invitation and wonderful hospitality during his sabbatical at which this work was done.

[1] Dagmar Bruß, J. Math. Phys. **43**, 4237 (2002).
[2] S. Hill and W.K. Wootters, Phys. Rev. Lett. **78**, 5022 (1997); W.K. Wootters, *ibid.* **80**, 2245 (1998).
[3] K.M. O'Connor and W.K. Wootters, Phys. Rev. A **63**, 052302 (2001).
[4] K.A. Dennison and W.K. Wootters, Phys. Rev. A **65**, 010301 (2002).
[5] D. Gunlycke, S. Bose, V.M. Kendon, and V. Vedral, Phys. Rev. A **64**, 042302 (2001).
[6] P. Zanardi, Phys. Rev. A **65**, 042101 (2002).
[7] T.J. Osborne and M.A. Nielsen, Phys. Rev. A **66**, 032110 (2002).
[8] A. Osterloh, Luigi Amico, G. Falci, and Rosario Fazio, Nature (London) **416**, 608 (2002).
[9] M.C. Gutzwiller, *Chaos in Classical and Quantum Mechanics* (Springer, New York, 1990).
[10] F. Haake, *Quantum Signature of Chaos*, 2nd ed. (Springer-Verlag, Berlin, 2001).
[11] A. Lakshminarayan, Phys. Rev. E **64**, 036207 (2001).
[12] J.N. Bandyopadhyay and A. Lakshminarayan, Phys. Rev. Lett. **89**, 060402 (2002).
[13] K. Zyczkowski and H-J. Sommers, J. Phys. A **34**, 7111 (2001).
[14] P. Jordan and E. Wigner, Z. Phys. **47**, 631 (1928); E. Lieb, T. Schultz, and D. Mattis, Ann. Phys. (N.Y.) **16**, 406 (1961); S. Sachdev, *Quantum Phase Transitions* (Cambridge University Press, Cambridge, 1999).
[15] A. Peres, *Quantum Theory: Concepts and Methods* (Kluwer Academic, Dordrecht, 1993); see J. Preskill, Lecture Notes at http://www.theory.caltech.edu/people/preskill/ph229
[16] C.H. Bennett, H.J. Bernstein, S. Popescu, and B. Schumacher, Phys. Rev. A **53**, 2046 (1996).
[17] F.M. Izrailev, in *Quantum Chaos: Between Order and Disor-*

der, edited by G. Casati and B. Chirikov (Cambridge University Press, Cambridge, 1995).
[18] P.G. Harper, Proc. Phys. Soc., London, Sect. A **68**, 874 (1955); **68**, 879 (1955).
[19] R. Artuso, G. Casati, F. Borgonovi, and L. Rebuzzini, Int. J. Mod. Phys. B **8**, 207 (1994).
[20] J. Schwinger, *Quantum Kinematics and Dynamics* (Benjamin, New York, 1970); J.H. Hannay and M.V. Berry, Physica D **1**, 267 (1980); M. Saraceno, Ann. Phys. (N.Y.) **199**, 37 (1990).
[21] P.B. Wiegmann, Prog. Theor. Phys. Suppl. **134**, 171 (1999).
[22] A. Iomin and S. Fishman, Phys. Rev. B **61**, 2085 (2000).
[23] P. Leboeuf, J. Kurchan, M. Feingold, and D.P. Arovas, Phys. Rev. Lett. **65**, 3076 (1990); R. Lima and D. Shepelyansky, *ibid.* **67**, 1377 (1991).
[24] M.L. Mehta, *Random Matrices* (Academic Press, New York, 1991).
[25] T.A. Brody, J. Flores, J.B. French, P.A. Mello, A. Pandey, and S.S.M. Wong, Rev. Mod. Phys. **53**, 385 (1981).
[26] N.R. Cerruti, A. Lakshminarayan, J.H. Lefebvre, and S. Tomsovic, Phys. Rev. E **63**, 016208 (2000); A. Lakshminarayan, N.R. Cerruti, and S. Tomsovic, *ibid.* **63**, 016209 (2000).
[27] M. Nielsen, e-print quant-ph/0208078.